

Orthodenticle and Kruppel homolog 1 regulate *Drosophila* photoreceptor maturation

Pierre Fichelson, Amira Brigui, and Franck Pichaud¹

Medical Research Council Laboratory for Molecular Cell Biology and Cell Biology Unit, and Department of Cell and Developmental Biology, University College London, London WC1E 6BT, United Kingdom

Edited by S. Lawrence Zipursky, University of California, Los Angeles, CA, and approved March 20, 2012 (received for review December 9, 2011)

Neurons present a wide variety of morphologies that are associated with their specialized functions. However, to date very few pathways and factors regulating neuronal maturation, including morphogenesis, have been identified. To address this issue we make use here of the genetically amenable developing fly photoreceptor (PR). Whereas this sensory neuron is specified early during retinal development, its maturation spans several days. During this time, this neuron acquires specialized membrane domains while undergoing extensive polarity remodeling. In this study, we identify a pathway in which the conserved homeobox protein Orthodenticle (Otd) acts together with the ecdysone receptor (EcR) to directly repress the expression of the transcription factor (TF) *Kruppel homolog 1* (*Kr-h1*). We demonstrate that this pathway is not required to promote neuronal specification but is crucial to regulate PR maturation. PR maturation includes the remodeling of the cell's epithelial features and associated apical membrane morphogenesis. Furthermore, we show that hormonal control coordinates PR differentiation and morphogenesis with overall development. This study demonstrates that during PR differentiation, transient repression of *Kr-h1* represents a key step regulating neuronal maturation. Down-regulation of *Kr-h1* expression has been previously associated with instances of neuronal remodeling in the fly brain. We therefore conclude that repression of this transcription factor represents a key step, enabling remodeling and maturation in a wide variety of neurons.

Neurons are highly polarized cells with complex shapes required for their specialized functions in the brain and in sensory organs. Whereas the mechanisms of neuronal specification are relatively well understood, much less is known about the molecular pathways that govern neuronal maturation, including the formation of specialized membrane domains and the acquisition of specific morphologies. The genetically amenable *Drosophila* photoreceptor (PR) is a striking example of how a postmitotic epithelial precursor cell can generate a light-sensitive neuron following a stepwise sequence of developmental events (Fig. S1). PR maturation comprises a step of polarity remodeling that consists of a 90° rotation of the cell's apicobasal axis (1–3). During polarity remodeling, PRs elongate by approximately 10-fold within the developing retina, and this is accompanied by the specification of two specialized membrane domains: the apical light-gathering rhabdomere and the supporting stalk membrane (ref. 1 and Fig. S1). To identify regulators of PR maturation, here we focused on the polarity remodeling of the PR soma. We identified the conserved homeobox-containing TF Otd (4) as a key factor that promotes PR maturation. Genome-wide profiling revealed that Otd is required for the transient repression of the zinc-finger-containing TF *Kr-h1* (5). We show that this transient repression results, at least in part, from the binding of both Otd and the ecdysone (20-hydroxyecdysone, 20E) receptor (EcR) to the *Kr-h1* promoter. Importantly, this transient repression is required to allow PR maturation to proceed normally. We conclude that the Otd/20E–*Kr-h1* pathway is part of a previously unrecognized molecular network that coordinates PR maturation with overall development of the animal.

Results

Otd Promotes PR Maturation. To monitor PR maturation and associated apicobasal polarity remodeling, we carried out live imaging using an E-cadherin::GFP transgene (Movie S1). Under these

experimental conditions, we observed resolution of the *zonula adherens* (ZA) of adjacent PRs by 44 h after puparium formation (APF) (compare Fig. 1A and C). Previous work has indicated that Otd is an important factor controlling both for *rhodopsin* expression and PR morphogenesis (6–10). However, it was not clear how Otd functions during PR maturation. To this end, we first determined Otd's pattern of expression and observed that it is expressed in third larval instar (L3) PRs (Fig. S24). Consistent with previous reports (6–8), we observed that Otd's expression is then maintained throughout PR development (Fig. S2A and B). However, Otd does not appear to regulate early steps of PR differentiation (Fig. S2C–H). We next assayed whether Otd was required to promote PR ZA remodeling (Movie S2). We found that *otd*^{UVI} PRs remodeled their ZA 16 h later than in a WT specimen: at 60 h APF instead of 44 h APF (Fig. 1A–D and F). *otd* is thus required for the correct timing of the onset of apicobasal polarity remodeling during PR maturation.

As the conserved polarity protein Crumbs (Crb) is known to be essential for PR ZA remodeling (3), we analyzed its pattern during PR maturation. By 48 h APF, WT PRs exhibited a strong apical accumulation of Crb (Fig. S3A–C). In contrast, between 24 and 48 h APF, the Crb signal was significantly lower in *otd*^{UVI} versus WT ommatidia (Fig. S3D). Whereas we consistently observed a strong and relatively specific reduction of Crb levels in *otd* mosaics analyzed at 48 h APF (Fig. S3E–H and Fig. S4A–F), this defect was only transient as Crb's levels were comparable in *otd* and WT PRs at 60 h APF (Fig. S3I–L). Consistent with defects in PR maturation and in agreement with previous reports (6–8), *otd*^{UVI} PRs exhibited defective elongation along the lens to brain axis (compare Fig. S5A and B; see Fig. 6H). As previously reported (7, 10), we could also detect rhabdomere morphogenesis defects with on average 1.8 cells harboring a split rhabdomere and 1.2 cells lacking a rhabdomere altogether per *otd*^{UVI} ommatidium (Fig. S5C–G). We also found that lack of *otd* leads to an overrepresentation of stalk membranes shorter than 1,500 nm (Fig. S1 and Fig. S5H).

Analysis of the *otd*-Dependent Transcriptome in Developing Retinas.

To identify the genes that are regulated by Otd during PR maturation, we compared total mRNAs extracted at 48 h APF from dissected WT, *otd*^{UVI}, and *otd*-overexpressing retinas (*GMR-otd*). Genes were considered to be differentially expressed if we detected a twofold difference in mRNA levels with a *P* value ≤ 0.05. Under these conditions, we identified 502 genes whose expression was affected by the loss of *otd* compared with WT retinas and 967 genes whose expression was modified by the overexpression of *otd* compared with WT retinas. Among the 502 genes affected by the loss of *otd*, 203 (40.4%) were affected in an opposite manner by the overexpression of *otd*, 294 (58.6%) were down-regulated, and 208

Author contributions: P.F., A.B., and F.P. designed research; P.F. and A.B. performed research; P.F., A.B., and F.P. contributed new reagents/analytic tools; P.F., A.B., and F.P. analyzed data; and P.F., A.B., and F.P. wrote the paper.

The authors declare no conflict of interest.

This article is a PNAS Direct Submission.

Freely available online through the PNAS open access option.

¹To whom correspondence should be addressed. E-mail: f.pichaud@ucl.ac.uk.

This article contains supporting information online at www.pnas.org/lookup/suppl/doi:10.1073/pnas.1120276109/-DCSupplemental.

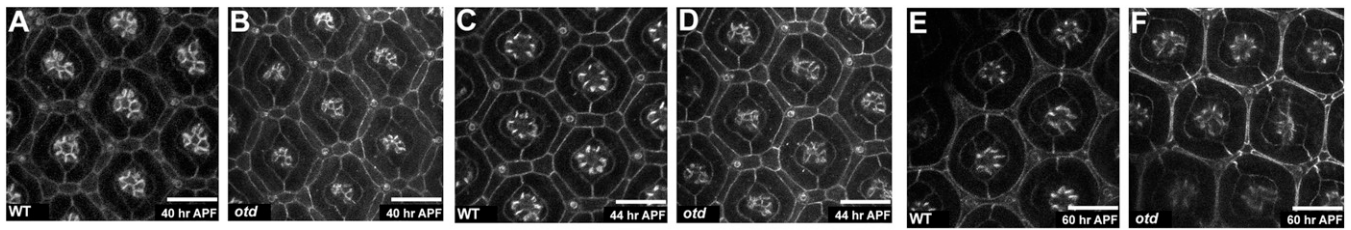


Fig. 1. *otd* is required for timely remodeling of PR ZA. (A–F) (Scale bars, 10 μm .) Stills taken from in vivo imaging of (A, C, and E) WT and (B, D, and F) *otd*^{UVI} eyes expressing E-cadherin::GFP. (A and B) 40 h APF, (C and D) 44 h APF, and (E and F) 60 h APF.

(41.4%) were up-regulated. We found minimal overlap between the *otd* targets we identified here and those previously identified at a later time point in development (96 h APF). Only 10 of the 502 genes were identified in ref. 11 (Table S1). This indicates that Otd regulates different sets of genes during different phases of PR maturation. The genes listed as part of the Otd-dependent transcriptome encode proteins with various functions, including modulators of phototransduction, neuronal activity, cell adhesion,

cytoskeleton, and transcription (Fig. S6A and Tables S2–S4). To validate our microarray approach, we generated *otd* clones and observed a clear decreased expression of three targets found to be down-regulated in the *otd* transcriptome [InaD, NinaC, and Choptin (Chp)] (Fig. S6 B–G). As expected, we also noted a 74-fold decrease in the levels of *otd* transcripts in *otd*^{UVI} versus WT retinas. Interestingly, among the genes whose transcription is differentially regulated in *otd* retinas, we found known targets of 20E signaling: *fushi tarazu transcription factor 1 (ftz-f1)*, *Ecdysone-induced protein 78C (Eip78C)*, and a modulator of this signaling pathway, *Kr-h1* (12–17). This observation suggests that, in concert with Otd, the systemic hormone 20E might be important to regulate PR maturation.

Otd Represses *Kr-h1* During PR Maturation. We next analyzed whether the delayed polarity remodeling in *otd* PRs could be due to a misregulation of *ftz-f1*, *Eip78C*, or *Kr-h1*. Both the *ftz-f1* and *Eip78C* mRNA levels are reduced in *otd* retinas (Table S4); however, their loss of function does not produce a PR phenotype. Compared with WT retinas, *Kr-h1* mRNA levels are increased by more than 14-fold in *otd* mutant retinas and reduced by 2-fold in *otd*-overexpressing retinas (Table S4). In agreement with these data, RT-qPCR performed on WT and *otd*^{UVI} retinas showed a 7-fold increase of *Kr-h1* mRNA abundance in mutant specimens (*Kr-h1* mRNA levels normalized to GAPDH mRNA levels; $n = 4$ independent mRNA extracts from *otd* and WT retinas, $P < 0.03$). To further test this regulation we determined *Kr-h1*'s expression pattern during PR development. Both in WT and *otd* retinas, *Kr-h1* is expressed in differentiating larval PRs and switched off soon after puparium formation (Fig. 2A and B). In WT PRs *Kr-h1* is reexpressed at 60 h APF (Fig. 2C), whereas its reexpression occurs ~ 12 h earlier in *otd* mutant compared with WT retina (Fig. 2D–F). Overall, our data therefore indicate that *otd* is required to transiently repress the expression of *Kr-h1* during PR maturation.

20E Signaling Regulates PR Maturation. *Kr-h1* is required both in the fly embryo and pupa for a proper response to 20E (15, 18) and our data suggest that both 20E and *Kr-h1* might be key regulators of PR maturation. We first tested whether pupal PRs are able to respond to 20E signaling using the *EcRE-LacZ* reporter (19). At 36 and 48 h APF, we detected β -galactosidase (β -Gal) expression both in WT and in *otd* ommatidia (Fig. 3A and B), indicating that PRs expressed the 20E receptor and responded to the 20E signal. However, our microarray data indicated that *otd* retinas failed to activate known 20E targets, suggesting defects in signal transduction. To test the hypothesis that suboptimal 20E signaling might be involved in generating the *otd* phenotype, we used RNAi to decrease the expression of *EcR*. Under these conditions, we observed a precocious accumulation of *Kr-h1* in PR nuclei at 48 h APF compared with control PRs (Fig. 3C and D). Interestingly, PRs also showed defective apical membrane maturation resembling the *otd* phenotype (Fig. 3E–H). 20E signaling thus acts as a repressor of *Kr-h1* expression and is required to promote PR maturation.

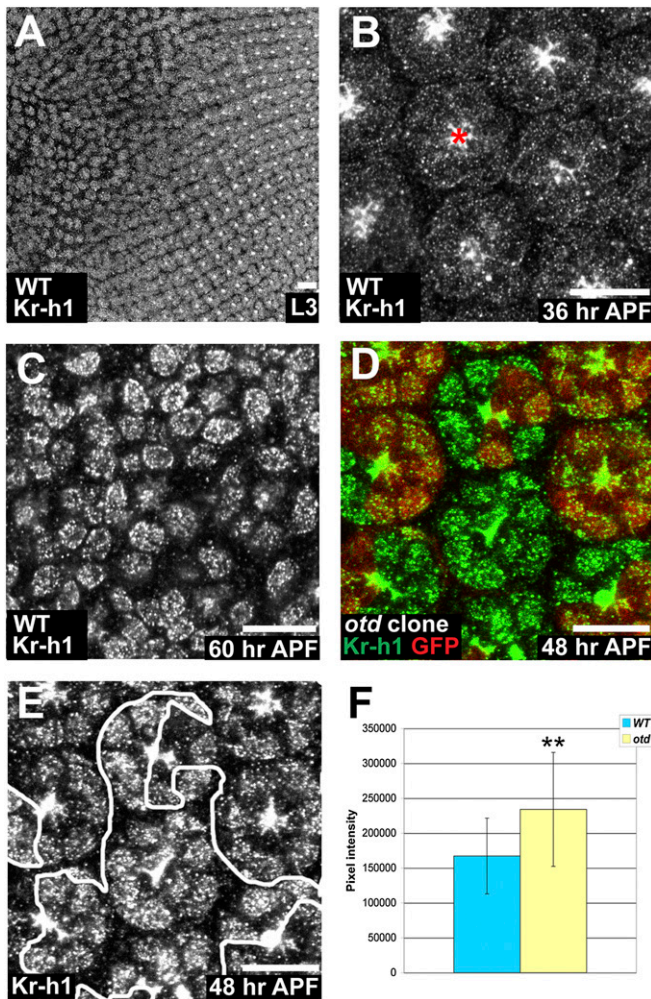


Fig. 2. *Kr-h1* expression is regulated by Otd in early pupal PRs. (A–E) (Scale bars, 10 μm .) (A–C) *Kr-h1* (gray) in WT. (A) L3 eye disk. (B) 36 h APF, red asterisk (*) indicates nonspecific apical staining. (C) 60 h APF. (D) *otd*² PRs. WT (red), *Kr-h1* (green). (E) *Kr-h1*. (F) Quantification of pixel intensity of *Kr-h1*. WT (blue) and *otd*² ommatidia (yellow). Asterisks indicate a statistically significant difference. $n = 93$ *otd* and 85 WT PR nuclei, $P \leq 10^{-5}$. Error bars represent SD.

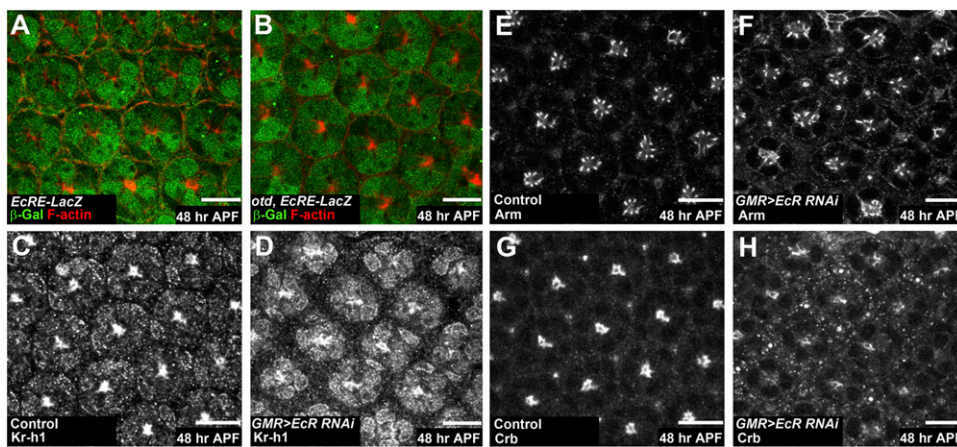


Fig. 3. 20E signaling is required for PR maturation. (A–H) 48 h APF. (Scale bars, 10 μ m.) (A and B) β -Gal (green), F-actin (red). *EcRE-LacZ* expression (A) in WT and (B) in *otd^{UVI}* PRs. (C, E, and G) Control specimen (*GMR-GAL4/UAS-gce RNAi*). (D, F, and H) Knockdown of the *EcR* (*GMR-GAL4/UAS-EcR RNAi*). (C–H) *Kr-h1* is in gray; (E and F) *Arm* is in gray; (G and H) *Crb* is in gray.

Otd and EcR Are both Required to Repress *Kr-h1* Transcription. To gain mechanistic insight into how Otd and 20E signaling are able to repress *Kr-h1*, we generated a reporter gene made of a 6-kb frag-

ment of the *Kr-h1* promoter cloned upstream of β -Gal (Fig. 4A). At 48 h APF, this reporter was weakly expressed in WT PRs and expressed at significantly stronger levels in *otd^{UVI}* PRs (Fig. 4B–G).

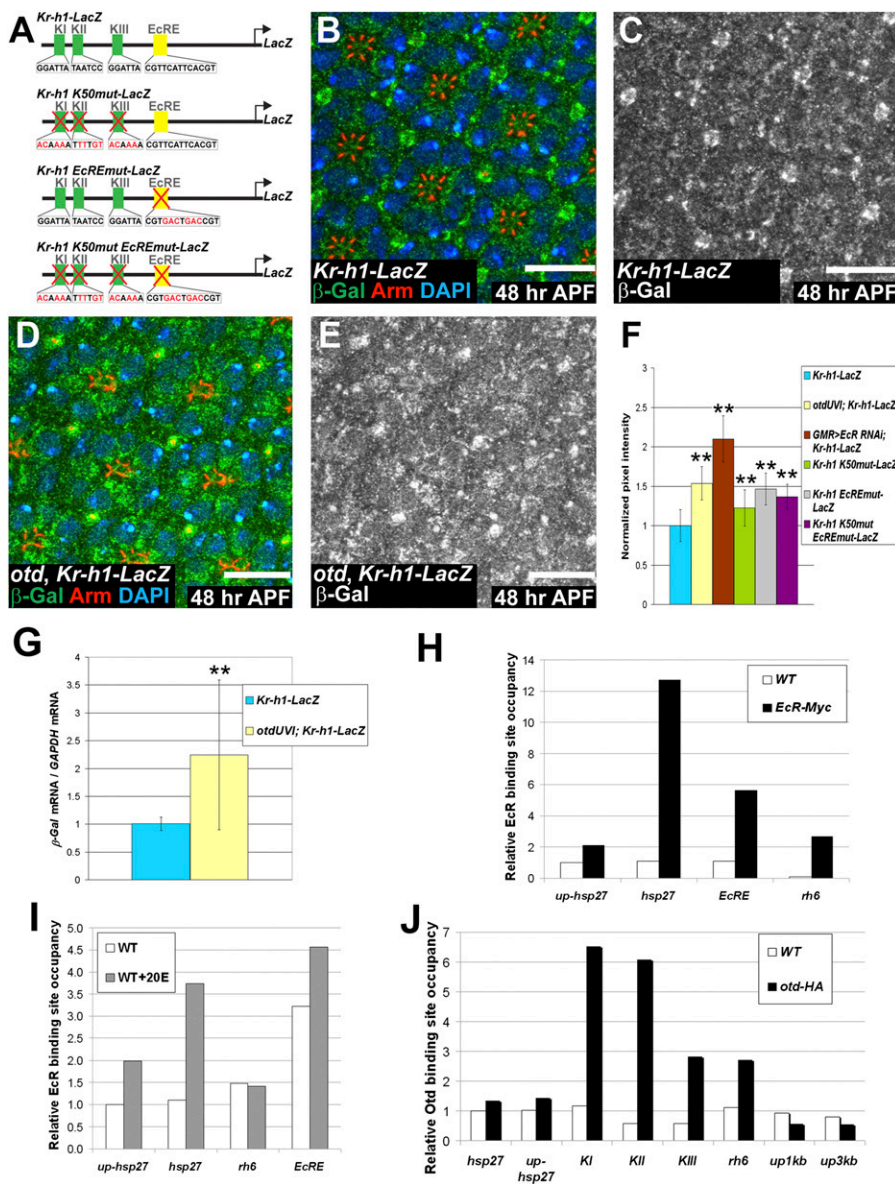


Fig. 4. Both Otd and EcR repress the transcription of *Kr-h1*. (A) Reporter genes generated to monitor *Kr-h1* regulation. KI–KIII represent the three K_{50} sites (green boxes) and EcRE represents the 20E receptor binding site (yellow box). Mutations and modified sequences are highlighted in red. (B–E) 48 h APF. (Scale bars, 10 μ m.) *Kr-h1-LacZ* expressed (B and C) in a WT and (D and E) in an *otd^{UVI}* background. (B and D) β -Gal (green), *Arm* (red), and DAPI (blue). (C and E) β -Gal (gray). (F) Quantification of pixel intensity of the β -Gal channel. WT ommatidia ($n = 192$) (blue), *otd^{UVI}* ommatidia ($n = 148$) (yellow), *GMR-GAL4/UAS-EcR RNAi* ($n = 52$) (brown), WT ommatidia expressing *Kr-h1 K50mut-LacZ*, ($n = 122$) (green), WT ommatidia expressing *Krh1 EcREmut-LacZ*, ($n = 132$) (gray), and WT ommatidia expressing *Krh1 K50mut EcREmut-LacZ*, ($n = 77$) (purple). Asterisks indicate statistically significant differences with WT ommatidia expressing *Kr-h1-LacZ*, $P \leq 10^{-17}$. Quantifications were performed in males. (G) qPCR quantification of *LacZ* mRNA normalized to GAPDH mRNA levels comparing *Kr-h1-LacZ* retinas (blue) and *otd^{UVI}*, *Kr-h1-LacZ* retinas (yellow) at 48 h APF. $n = 9$ independent mRNA extracts from *otd* and WT retinas, $P \leq 0.04$. Error bars represent SD. (H–J) Representative experiment of $n \geq 2$ (H) ChIP carried out using an anti-MYC antibody on WT (white) and *EcR-MYC*-overexpressing cells (black). (I) ChIP carried out using an anti-EcR antibody on nontreated (white) and 20E treated WT cells (gray). (J) ChIP carried out using an anti-HA antibody on WT (white) and *otd-HA*-overexpressing cells (black).

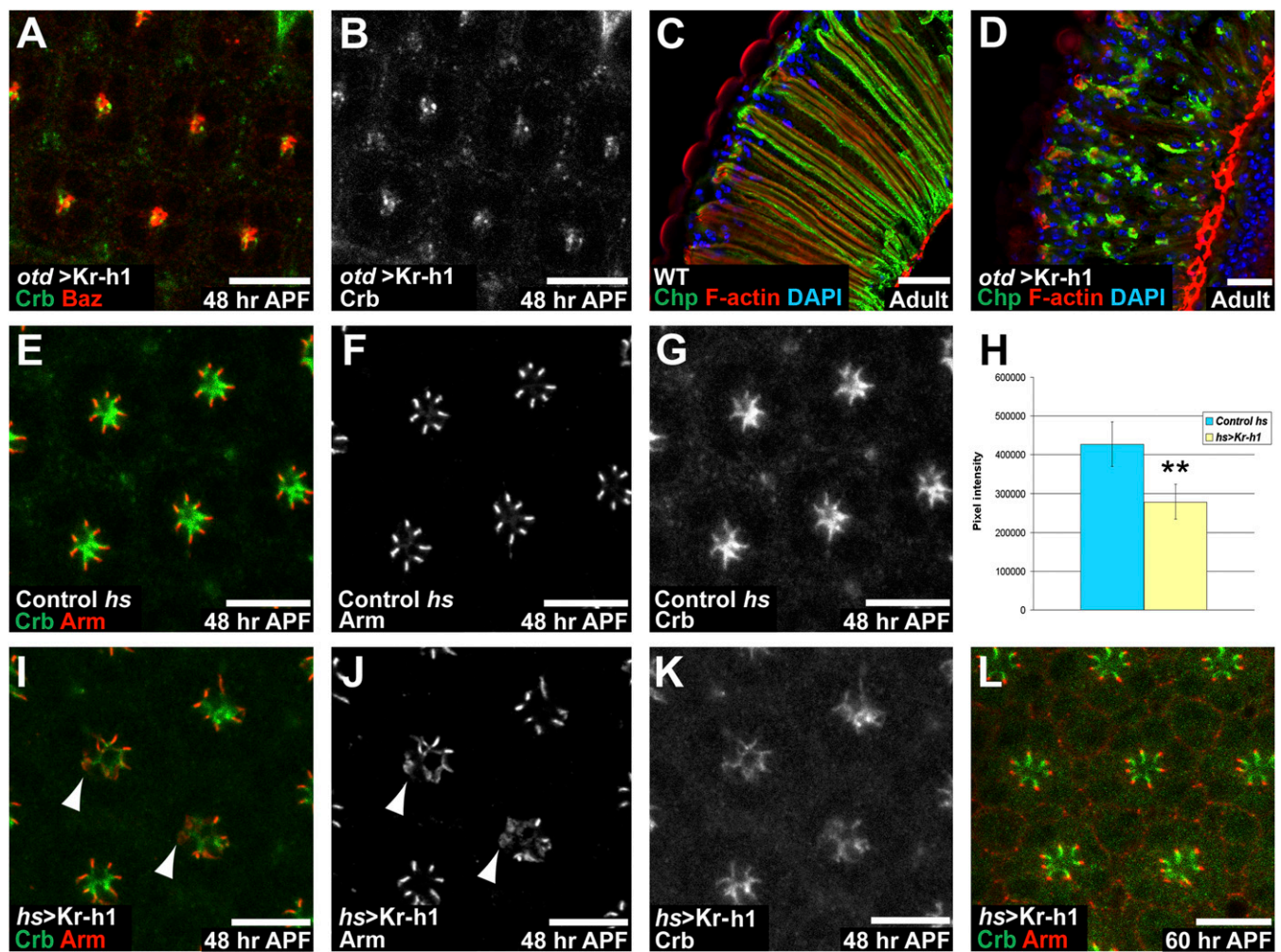


Fig. 5. Ectopic Kr-h1 is sufficient to affect PR maturation. (A and B) *otd-Gal4/UAS-Kr-h1*, at 48 hr APF. (Scale bars, 10 μ m.) (A) Crb (green) and Baz (red). (B) Crb (gray). (C and D) Cryosection of adult retinas. Chp (green), phalloidin (red), and DAPI (blue). (Scale bars, 20 μ m.) (C) WT retina and (D) *otd-Gal4/UAS-Kr-h1* retina. (E–G and I–L) (Scale bars, 10 μ m.) (E, I, and L) Crb (green), Arm (red). (F and J) Arm (gray). (G and K) Crb (gray). (E–G) Control (*hs-Gal4*) treated as for the assay. (H) Quantification of pixel intensity of the Crb channel comparing control (*hs-Gal4*, blue) and *hs-Gal4/UAS-Kr-h1* retinas (yellow). Asterisks indicate a statistically significant difference. $n = 34$ *otd* and 47 WT ommatidia, $P \leq 10^{-19}$. (I–L) *hs-Gal4/UAS-Kr-h1*. (I–K) 48 hr APF. (I and J) Arrowheads indicate mislocalized Arm. (L) 60 hr APF.

In addition, we found that *Kr-h1* mRNA and protein levels were also significantly higher in *otd* compared with WT PRs (Fig. 2D–F). Furthermore, we observed a strong level of expression of *Kr-h1* and *Kr-h1-LacZ* in PRs when knocking down the EcR subunit of the 20E receptor (Figs. 3C and D and 4F). This observation raised the possibility that both Otd and 20E might directly regulate *Kr-h1*. Consistent with this hypothesis, three putative Otd binding sites (K_{50} sites, named KI–KIII) and one 20E receptor binding site (named EcRE) (17) are present within the 6 kb of the *Kr-h1* promoter region used in our reporter assay. To test whether these sites are functional in vivo, we mutated the K_{50} sites and the 20E receptor binding site, independently or in combination in the same promoter (Fig. 4A). In all cases, these mutations resulted in stronger expression of the corresponding transgenes compared with the WT transgene (Fig. 4F). Both the K_{50} and the EcR binding sites are therefore functional and required to repress the transcription of *Kr-h1* in vivo, consistent with a regulation of *Kr-h1* by Otd and the 20E receptor.

To gain further insight into the mechanisms underlying the regulation of *Kr-h1* transcription by EcR and Otd, we performed chromatin-immunoprecipitation (ChIP) experiments in S2 cells. As controls, we used *hsp27*, a known 20E target whose promoter does not contain K_{50} binding sites and *rhodopsin 6* (*rh6*), a known Otd target devoid of any identified EcR binding site. In separate assays

we were able to immunoprecipitate both endogenous EcR and transfected EcR-MYC. Under these conditions, qPCR analysis revealed an important enrichment of DNA fragments containing the known EcR binding site of the *hsp27* promoter, but no enrichment of DNA fragments of regions located 1 kb upstream of the EcR binding site in the *hsp27* promoter (*up-hsp27*, Fig. 4H and I) (20). Similarly we did not detect any major enrichment of DNA fragments containing the *rh6* regulatory regions, reflecting the specificity of the ChIP assay. Importantly, and consistent with our model, we clearly detected the EcRE domain of the endogenous *Kr-h1* promoter (Fig. 4H and I). In addition, supplementing the culture medium with 20E before ChIP led to increased amounts of DNA fragments containing the EcR binding site of both *hsp27* and *Kr-h1* regulatory regions, indicating that the presence of the 20E increased the affinity of EcR for the *Kr-h1* promoter (Fig. 4I). Similarly, we performed Otd ChIP following transfection of S2 cells with *otd-HA*. Under these conditions, we did not detect any enrichment of DNA fragments of the *hsp27* promoter or of DNA fragments located 1 kb (*up1kb*) and 3 kb (*up3kb*) upstream of the KI site in the *Kr-h1* regulatory sequences (Fig. 4J). Importantly, this set of experiments revealed a clear and reproducible enrichment of *rh6* regulatory regions and of the KI, KII, and KIII regions of the endogenous *Kr-h1* promoter (Fig. 4J). These ChIP data thus indicate that both Otd

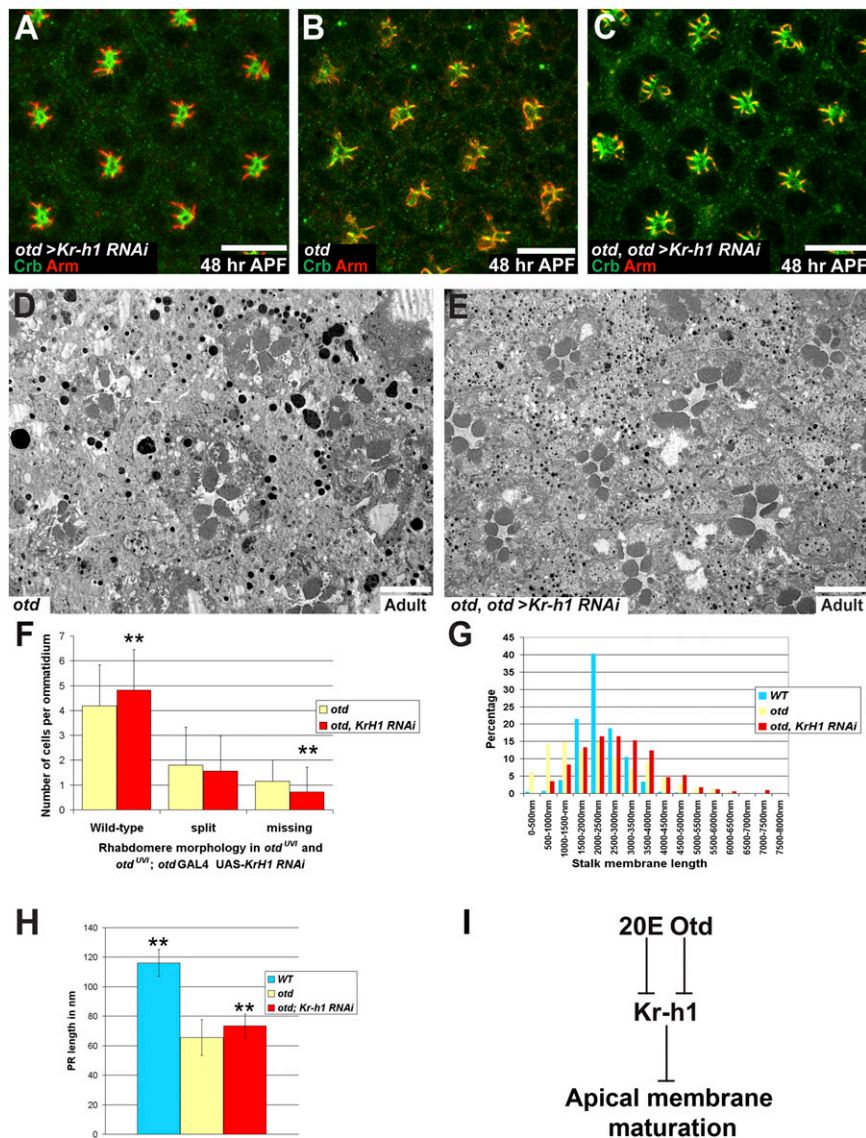


Fig. 6. Knocking down *Kr-h1* in an *otd* background partially suppresses PR maturation defects. (A–C) Crb (green), Arm (red), ommatidia at 48 h APF. (Scale bars, 10 μ m.) (A) *otd-Gal4/UAS-Kr-h1 RNAi*. (B) *otd^{UV1}/Y; otd-Gal4/SM6:TM6* PRs. (C) *otd^{UV1}/Y; otd-Gal4/UAS-Kr-h1 RNAi*. (D and E) (Scale bars, 5 μ m.) (D) *otd^{UV1}/Y; otd-Gal4/SM6:TM6* and (E) *otd^{UV1}/Y; otd-Gal4/UAS-Kr-h1 RNAi*. (F) Rhabdomere morphology in *otd^{UV1}/Y; otd-Gal4/SM6:TM6* (yellow) and in an *otd^{UV1}/Y; otd-Gal4/UAS-Kr-h1 RNAi* background (red). Asterisks indicate a statistically significant difference. $n = 1,122$ *otd* PRs and 816 *otd + Kr-h1 RNAi* PRs, $P \leq 10^{-3}$. (G) Stalk membrane length in WT PRs (blue), in *otd^{UV1}/Y; otd-Gal4/SM6:TM6* (yellow), and in *otd^{UV1}/Y; otd-Gal4/UAS-Kr-h1 RNAi* PRs (red). (H) PR length over several Z-sections of WT PRs (blue), in *otd^{UV1}/Y; otd-Gal4/SM6:TM6* (yellow), and in *otd^{UV1}/Y; otd-Gal4/UAS-Kr-h1 RNAi* PRs (red). Asterisks indicate a statistically significant difference. $n = 30$ PRs for each genotype $P \leq 0.0055$. (I) Working model.

and EcR can bind to the three K_{50} (KI–III) and EcRE, respectively, that we have identified in the *Kr-h1* regulatory promoter region.

Transient Repression of *Kr-h1* Is Required to Promote PR Maturation. Together our data are compatible with a model where both Otd and EcR regulate the transcription of *Kr-h1* at the onset of PR remodeling. To test whether ectopic expression of *Kr-h1* might interfere with PR maturation, we overexpressed *Kr-h1* under the control of the *otd* promoter. The pattern of Otd was unaffected under these conditions, but we observed that at 48 h APF, PR maturation was strongly affected (Fig. 5A–D), indicating that transient repression of *Kr-h1* is required for PR maturation to proceed normally. This finding was confirmed by providing a pulse of *Kr-h1* at 24 h APF and dissecting samples at 48 h APF. Under these conditions, PR maturation was impaired (Fig. 5E–L) and resembled the *otd* phenotype. If part of *otd*'s function is to transiently repress *Kr-h1*, down-regulating *Kr-h1* in an *otd* mutant retina should suppress the *otd*

phenotype. When reducing *Kr-h1* levels in an *otd* background using two independent RNAi lines, we observed a partial suppression of the *otd* phenotype (Fig. 6A–H). These data indicate that *Kr-h1* is an important downstream target of Otd whose transient repression is required for PR maturation to proceed normally.

Discussion

Transcriptional Regulation During PR Maturation. Whereas the mechanisms underlying neuronal specification during development are relatively well described, how the wide variety of neuronal shapes and functions are produced during development remains poorly understood. Here, we use the developing *Drosophila* PR as a model system and report a genetic and molecular pathway that consists of Otd, *Kr-h1*, and EcR. In this pathway, Otd and EcR both converge to transiently repress the expression of *Kr-h1* and this transient repression is required for correct PR maturation (Fig. 6I). We have identified three Otd binding sites as well as one EcR

binding site in the *Kr-h1* promoter and our data indicate that both Otd and EcR regulate this gene's transcription at least in part by binding directly to these sites. However, the fact that the levels of expression of the WT *Kr-h1* reporter gene in *otd* mutant retinas were stronger than the levels of expression of the same reporter mutated for all three putative K₅₀ sites also argues for indirect regulation. Another nonexclusive possibility could be that Otd regulates *Kr-h1* through noncanonical sites in addition to the K₅₀ sites we mutated. Similarly, our promoter dissection indicates that the transcription of *Kr-h1* is also likely to be regulated both directly and indirectly by the 20E receptor.

Kr-h1 Exhibits Antimorphogenetic Activity in Fly Neurons. Previous work in the hemimetabolous insects, thrips, *Thysanoptera*, and in the beetle *Tribolium castaneum*, suggest that Kr-h1 could be involved in mediating antimetamorphic signals (21, 22). In addition, studies in *Drosophila* show that Kr-h1 orchestrates 20E-regulated transcriptional pathways during embryogenesis and metamorphosis (15, 16). It is therefore tempting to speculate that Kr-h1 could play an important role transducing systemic hormone signaling at the cellular level. In the adult honeybee workers, increased levels of Kr-h1 have been associated with a change of behavior, from nursing to foraging, as a response to pheromone signals emanating from the queen (23). Interestingly, these changes of levels of expression take place at the time of neurite outgrowth and synapse formation in the mushroom body part of the bee brain (24), suggesting that Kr-h1 could control neuronal morphogenesis. Moreover, in the fly, the overexpression of Kr-h1 was shown to induce axon path-finding defects in larval neurons (25). Interestingly, in *Drosophila* mushroom body neurons, *Kr-h1* is down-regulated both at the

time of initial morphological differentiation and during metamorphic neurite remodeling, indicating that the levels of Kr-h1 need to be down-regulated to allow neuronal morphogenesis (18). In a consistent manner, the overexpression of Kr-h1 is sufficient to block mushroom body neuron morphogenesis and to inhibit axon remodeling during metamorphosis. Kr-h1 thus appears to present an antimorphogenetic activity in developing and remodeling neurons. Our work identifies a pathway where the regulation of *Kr-h1* results both from systemic 20E signaling and PR-specific expression of Otd. We propose that this mode of regulation of *Kr-h1* resulting from the combination of a neuron subtype-specific TF and 20E signaling is likely to be broadly relevant for neuronal maturation and remodeling in *Drosophila*.

Materials and Methods

Fly crosses were maintained at 25° unless specified. For each microarray hybridization and RT-PCR, 60 staged retinas were used. ChIP experiments were performed in S2 cells using *pAct-EcR-MYC* (26) and *pAct-otd-HA* (this work) combined to mouse anti EcR-B1 (AD4.4, DSHB), mouse anti-MYC (sc-40) or rat anti-HA (3F10, Roche). Whole-mount retinas were prepared as described in (27). Detailed experimental methods regarding the molecular biology, ChIP, immunofluorescence, and electron microscopy are provided in *SI Materials and Methods*.

ACKNOWLEDGMENTS. We thank T. Cook, Y. Fengwei, and E. Wimmer for reagents; M. Hubank, N. Jina, K. Pearce, and M. Rahman for their help with the microarray analysis; and F. Bernard, J. Burden, A. -L. Cattin, Y. Fujita, M. Kajita, and B. Pourcet for technical advice. P.F. was supported by a European Molecular Biology Organization Long-Term Fellowship and by a Medical Research Council (MRC) Career Development Fellowship (CDF). A.B. is supported by an MRC CDF. Work in F.P.'s laboratory is funded by the MRC.

- Longley RL, Jr., Ready DF (1995) Integrins and the development of three-dimensional structure in the *Drosophila* compound eye. *Dev Biol* 171:415–433.
- Izaddoost S, Nam SC, Bhat MA, Bellen HJ, Choi KW (2002) *Drosophila* Crumbs is a positional cue in photoreceptor adherens junctions and rhabdomeres. *Nature* 416:178–183.
- Walther RF, Pichaud F (2010) Crumbs/DaPKC-dependent apical exclusion of Bazooka promotes photoreceptor polarity remodeling. *Curr Biol* 20:1065–1074.
- Finkelstein R, Perrimon N (1990) The orthodenticle gene is regulated by bicoid and torso and specifies *Drosophila* head development. *Nature* 346:485–488.
- Schuh R, et al. (1986) A conserved family of nuclear proteins containing structural elements of the finger protein encoded by Krüppel, a *Drosophila* segmentation gene. *Cell* 47:1025–1032.
- Tahayato A, et al. (2003) Otd/Crx, a dual regulator for the specification of ommatidia subtypes in the *Drosophila* retina. *Dev Cell* 5:391–402.
- Vandendries ER, Johnson D, Reinke R (1996) Orthodenticle is required for photoreceptor cell development in the *Drosophila* eye. *Dev Biol* 173:243–255.
- McDonald EC, et al. (2010) Separable transcriptional regulatory domains within Otd control photoreceptor terminal differentiation events. *Dev Biol* 347:122–132.
- Johnston RJ, Jr., et al. (2011) Interlocked feedforward loops control cell-type-specific Rhodopsin expression in the *Drosophila* eye. *Cell* 145:956–968.
- Mishra M, et al. (2010) Pph13 and orthodenticle define a dual regulatory pathway for photoreceptor cell morphogenesis and function. *Development* 137:2895–2904.
- Ranade SS, et al. (2008) Analysis of the Otd-dependent transcriptome supports the evolutionary conservation of CRX/OTX/OTD functions in flies and vertebrates. *Dev Biol* 315:521–534.
- Russell SR, Heimbeck G, Goddard CM, Carpenter AT, Ashburner M (1996) The *Drosophila* Eip78C gene is not vital but has a role in regulating chromosome puffs. *Genetics* 144:159–170.
- Broadus J, McCabe JR, Endrizzi B, Thummel CS, Woodard CT (1999) The *Drosophila* beta FTZ-F1 orphan nuclear receptor provides competence for stage-specific responses to the steroid hormone ecdysone. *Mol Cell* 3:143–149.
- Woodard CT, Baehrecke EH, Thummel CS (1994) A molecular mechanism for the stage specificity of the *Drosophila* prepupal genetic response to ecdysone. *Cell* 79:607–615.
- Pecasse F, Beck Y, Ruiz C, Richards G (2000) Krüppel-homolog, a stage-specific modulator of the prepupal ecdysone response, is essential for *Drosophila* metamorphosis. *Dev Biol* 221:53–67.
- Beck Y, Pecasse F, Richards G (2004) Krüppel-homolog is essential for the coordination of regulatory gene hierarchies in early *Drosophila* development. *Dev Biol* 268:64–75.
- Gauhar Z, et al. (2009) Genomic mapping of binding regions for the Ecdysone receptor protein complex. *Genome Res* 19:1006–1013.
- Shi L, et al. (2007) Roles of *Drosophila* Krüppel-homolog 1 in neuronal morphogenesis. *Dev Neurobiol* 67:1614–1626.
- Kozlova T, Thummel CS (2003) Essential roles for ecdysone signaling during *Drosophila* mid-embryonic development. *Science* 301:1911–1914.
- Sawatsubashi S, et al. (2004) Ecdysone receptor-dependent gene regulation mediates histone poly(ADP-ribosylation). *Biochem Biophys Res Commun* 320:268–272.
- Minakuchi C, Namiki T, Shinoda T (2009) Krüppel homolog 1, an early juvenile hormone-response gene downstream of Methoprene-tolerant, mediates its anti-metamorphic action in the red flour beetle *Tribolium castaneum*. *Dev Biol* 325:341–350.
- Minakuchi C, Tanaka M, Miura K, Tanaka T (2011) Developmental profile and hormonal regulation of the transcription factors broad and Krüppel homolog 1 in hemimetabolous thrips. *Insect Biochem Mol Biol* 41:125–134.
- Grozinger CM, Robinson GE (2007) Endocrine modulation of a pheromone-responsive gene in the honey bee brain. *J Comp Physiol A Neuroethol Sens Neural Behav Physiol* 193:461–470.
- Grozinger CM, Sharabash NM, Whitfield CW, Robinson GE (2003) Pheromone-mediated gene expression in the honey bee brain. *Proc Natl Acad Sci USA* 100(Suppl 2):14519–14525.
- Kraut R, Menon K, Zinn K (2001) A gain-of-function screen for genes controlling motor axon guidance and synaptogenesis in *Drosophila*. *Curr Biol* 11:417–430.
- Kirilly D, et al. (2011) Intrinsic epigenetic factors cooperate with the steroid hormone ecdysone to govern dendrite pruning in *Drosophila*. *Neuron* 72:86–100.
- Walther RF, Pichaud F (2006) Immunofluorescent staining and imaging of the pupal and adult *Drosophila* visual system. *Nat Protoc* 1:2635–2642.